Small-x Helicity Global Analysis: Now With Polarized pp Data

NICHOLAS BALDONADO

NEW MEXICO STATE UNIVERSITY

NM STATE BE BOLD. Shape the Future.®

This work is supported by the U.S. Department of Energy, Office of Science, Office of Nuclear Physics, within the framework of the Saturated Glue (SURGE) Topical Collaboration, subcontract #32095

SURGE COLLABORATION

Proton Spin Puzzle and Small-x

- Proton Spin ≡ ½, Experimental Measurement of spin coming from partons ≠ ½
- Jaffe-Manohar sum rule [1]: $S_q + L_q + S_G + L_G = \frac{1}{2}$

$$S_q(Q^2) = \frac{1}{2}\int_0^1 dx\ \Delta\Sigma(x, Q^2), \quad S_G(Q^2) = \int_0^1 dx\ \Delta G(x, Q^2)$$

- Experimental data only exists for a range of values $x \in [x_{min}, 1]$

"Knockout" DIS at Large-x

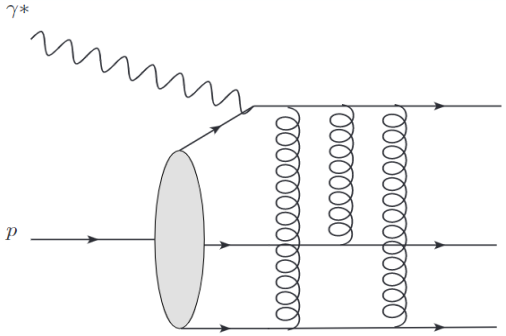

$$x = \frac{Q^2}{s + Q^2} \sim \frac{Q^2}{E_{CM}^2} \sim \frac{1}{m\,\Delta t_{Ioffe}}$$

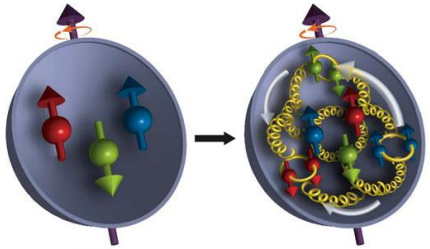

"Dipole" DIS at Small-x

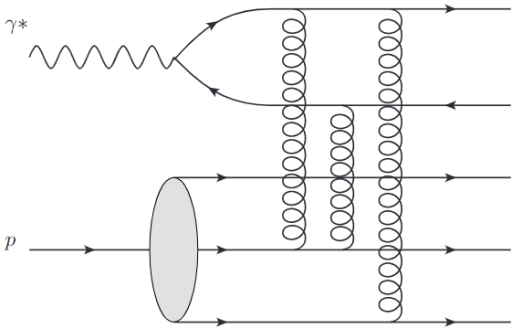

At small-x and with large Ioffe time our degrees of freedom change from quarks and gluons to eikonal Wilson Lines, and the proton appears very dense and frozen.

Sub-Eikonal Corrections and Double Logs

Unpolarized Wilson Line

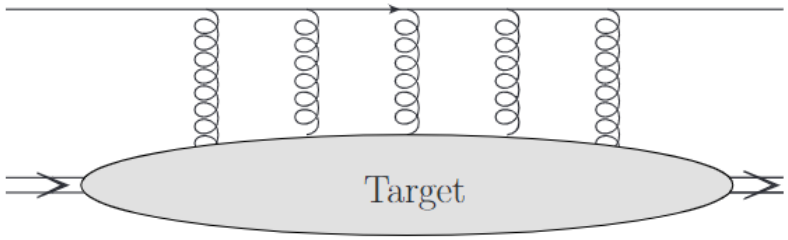

$$V_{\underline{0}} = \mathcal{P}\exp\left[ig\int_{-\infty}^{+\infty} dx^- A^+\left(x^+ = 0, x^-, \underline{x}_0\right)\right]$$

Polarized Wilson Line

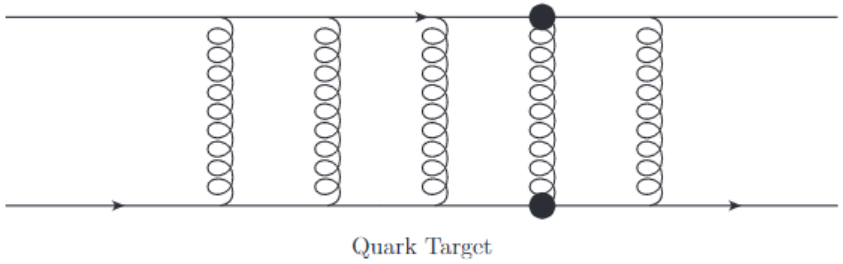

$$\left(V_{\underline{x}}^{pol}\right)^g \propto \int_{-\infty}^{\infty} dx^-\, V_{\underline{x}}[+\infty, x^-] F^{12}\left(x^-, \underline{x}\right) V_{\underline{x}}[x^-, -\infty]$$

$$\frac{\partial}{\partial Y}$$

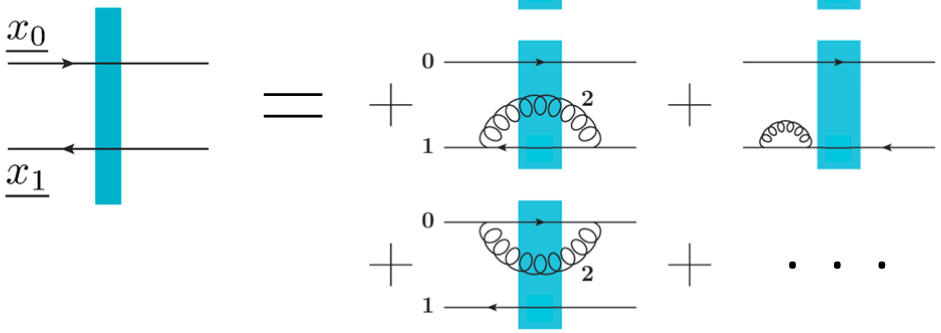

Radiative Corrections

↓

Small-x Evolution

Unpolarized evolution: $\alpha_s \ln\frac{1}{x} \sim 1$

Polarized evolution: $\alpha_s \ln^2\frac{1}{x} \sim 1$

KPS-CTT Evolution and Helicity Distribution

KPS-CTT = Kovchegov-Pitonyak-Sievert-Cougoulic-Tarasov-Tawabutr

$$Q_{10}(zs) \equiv \frac{1}{2N_c}\,\mathrm{Re}\left\langle\!\!\left\langle \mathrm{T\,tr}\left[V_{\underline{0}}\,V_{\underline{1}}^{\mathrm{pol}[1]\,\dagger}\right] + \mathrm{T\,tr}\left[V_{\underline{1}}^{\mathrm{pol}[1]}\,V_{\underline{0}}^{\dagger}\right]\right\rangle\!\!\right\rangle(zs)$$

$$G_{10}^{i}(zs) \equiv \frac{1}{2N_c}\left\langle\!\!\left\langle \mathrm{tr}\left[V_{\underline{0}}^{\dagger}\,V_{\underline{1}}^{i\,\mathrm{G}[2]} + \left(V_{\underline{1}}^{i\,\mathrm{G}[2]}\right)^{\dagger}\,V_{\underline{0}}\right]\right\rangle\!\!\right\rangle(zs)$$

$\cdots$

Polarized dipole amplitudes are various combinations of polarized and unpolarized Wilson lines [2-4].

$$\begin{aligned}
Q_f(x_{10}^2, zs) &\sim Q_f^{(0)}(x_{10}^2, zs) + \iint\left[2\tilde{G} + \tilde{\Gamma} + Q_f - \bar{\Gamma}_f + 2\Gamma_2 + 2G_2\right] + \iint\left[Q_f + 2G_2\right]\\
\bar{\Gamma}_f(x_{10}^2, x_{21}^2, z's) &\sim Q_f^{(0)}(x_{10}^2, z's) + \iint\left[2\tilde{G} + 2\tilde{\Gamma} + Q_f - \bar{\Gamma}_f + 2\Gamma_2 + 2G_2\right] + \iint\left[Q_f + 2G_2\right]\\
\tilde{G}(x_{10}^2, zs) &\sim \tilde{G}^{(0)}(x_{10}^2, zs) + \iint\left[3\tilde{G} + \tilde{\Gamma} + 2G_2 + \Gamma_2 - \bar{\Gamma}_f\right] - \iint\left[Q_f + 2G_2\right]\\
\tilde{\Gamma}(x_{10}^2, x_{21}^2, z's) &\sim \tilde{G}^{(0)}(x_{10}^2, z's) + \iint\left[3\tilde{G} + \tilde{\Gamma} + 2G_2 + \Gamma_2 - \bar{\Gamma}_f\right] - \iint\left[Q_f + 2G_2\right]\\
G_2(x_{10}^2, zs) &\sim G_2^{(0)}(x_{10}^2, zs) + \iint\left[\tilde{G} + 2G_2\right]\\
\Gamma_2(x_{10}^2, x_{21}^2, z's) &\sim G_2^{(0)}(x_{10}^2, z's) + \iint\left[\tilde{G} + 2G_2\right]
\end{aligned}$$

(Large-N_c&N_f)

$$\boldsymbol{\Delta G} \propto G_2$$

$$\boldsymbol{\Delta\Sigma} \propto -\int\int\left[Q_f + 2G_2\right]$$

$$\boldsymbol{\Delta q_f^{NS}} \propto \int\int\left[G_f^{NS}\right]$$

$$\boldsymbol{A_{\parallel}^{DIS}} \propto \boldsymbol{A_1} \propto \boldsymbol{g_1^p} \propto -\int\int\left[Q_f + 2G_2\right]$$

$\boldsymbol{Q_f^{(0)}, \tilde{G}^{(0)}, G_2^{(0)}, G_f^{NS\,(0)}}$ $(x \approx 0.1)$ ➡ **KPS-CTT [5]** ➡ $\boldsymbol{\Delta G, \Delta\Sigma, \Delta q_f^{NS}, g_1}$ $(x \ll 0.1)$

Global Analysis: Bayesian-MC Analysis

$$G^{(0)} \approx a\eta + bs_{10} + c$$

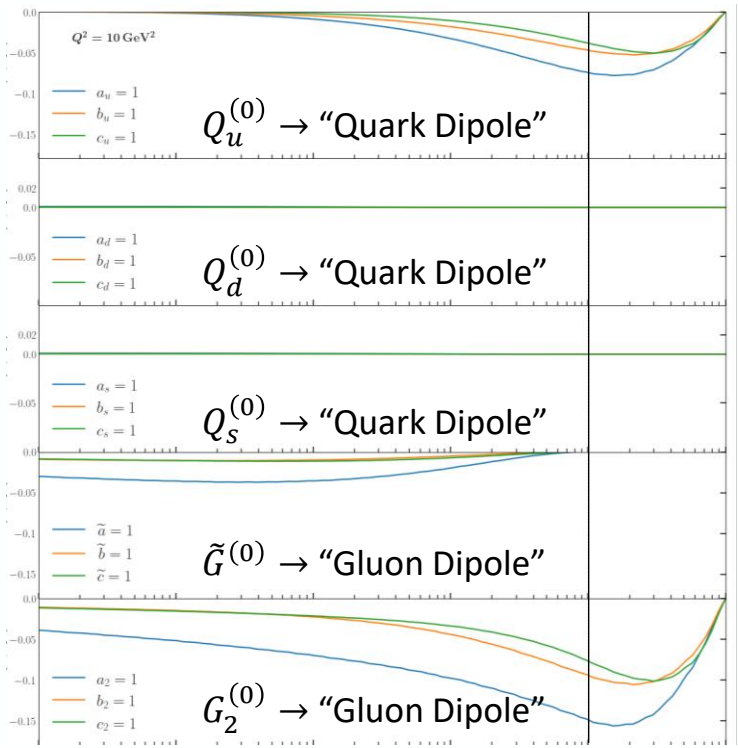

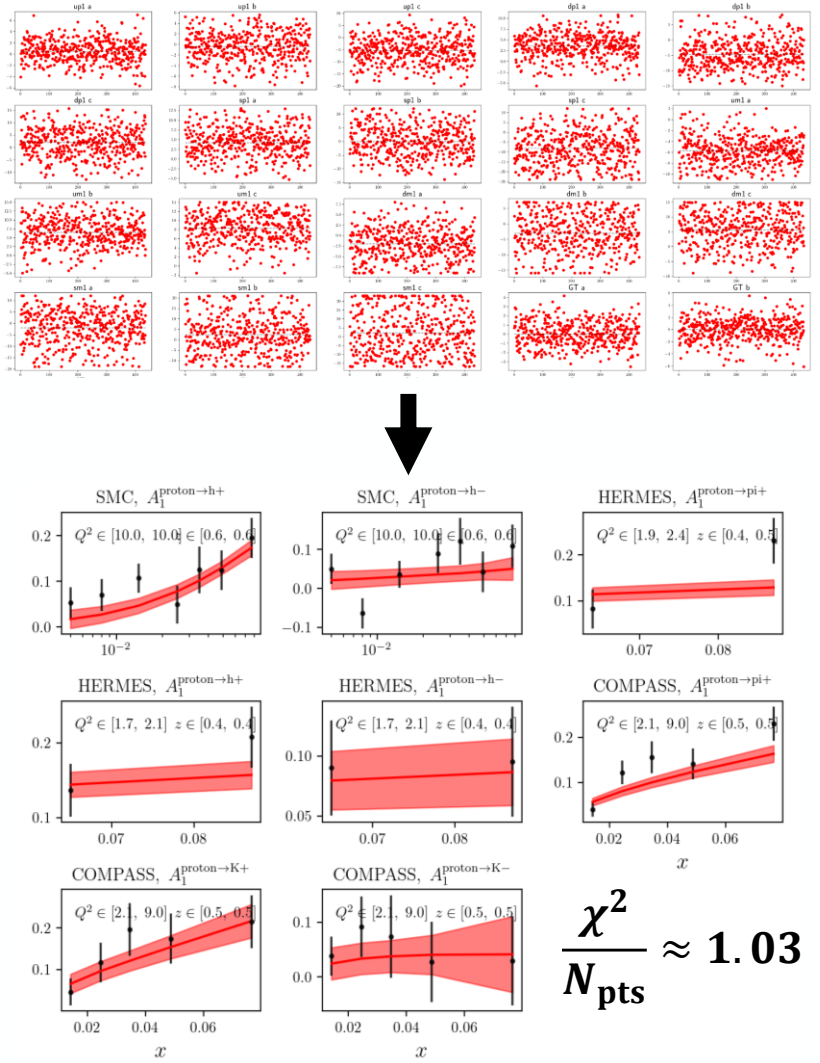

$$\frac{\chi^2}{N_{\mathrm{pts}}} \approx 1.03$$

- Compute Full Evolution from any parameter.
- Chi-squared optimization for DIS and SIDIS data.

Global Analysis: Success and Setback with SIDIS

SIDIS data improves the first analysis [6] and allows us to separate quark flavor hPDFs, Δq_f, from $\Delta\Sigma$.

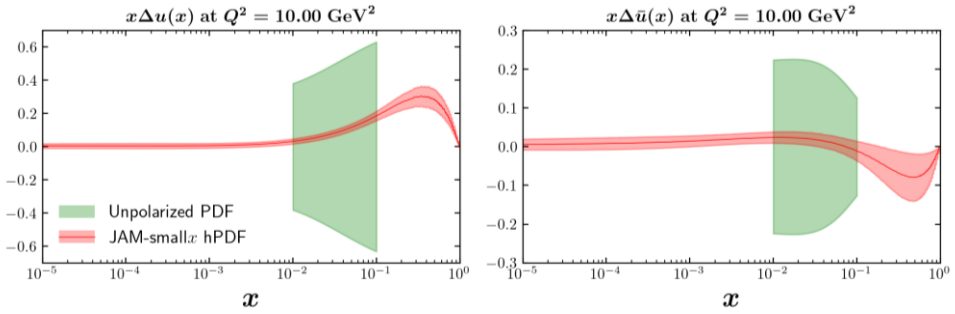

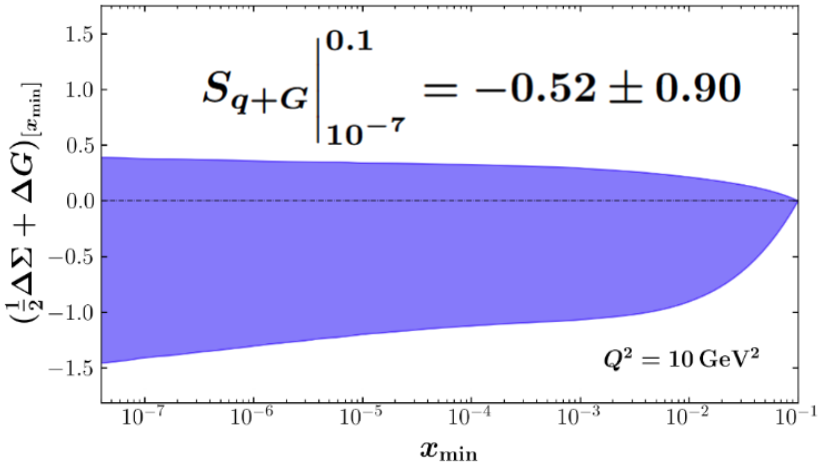

$$\lim_{x\to 0} g_1^p \sim \lim_{x\to 0} \Delta\Sigma \sim \lim_{x\to 0} \Delta G \sim \left(\frac{1}{x}\right)^{\alpha_h}$$

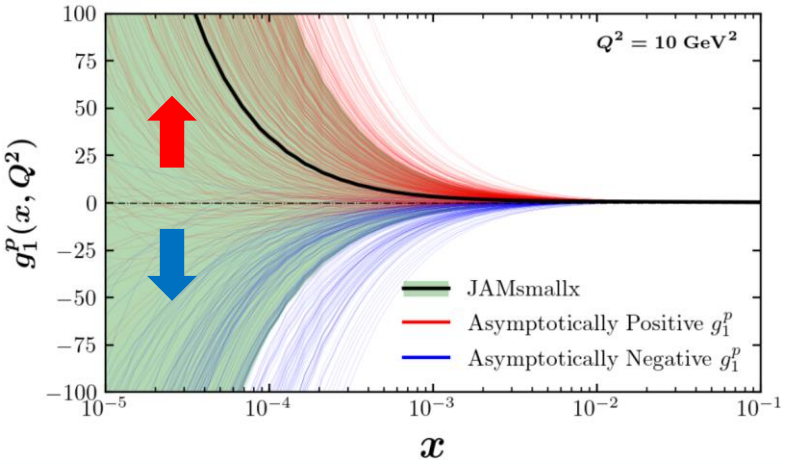

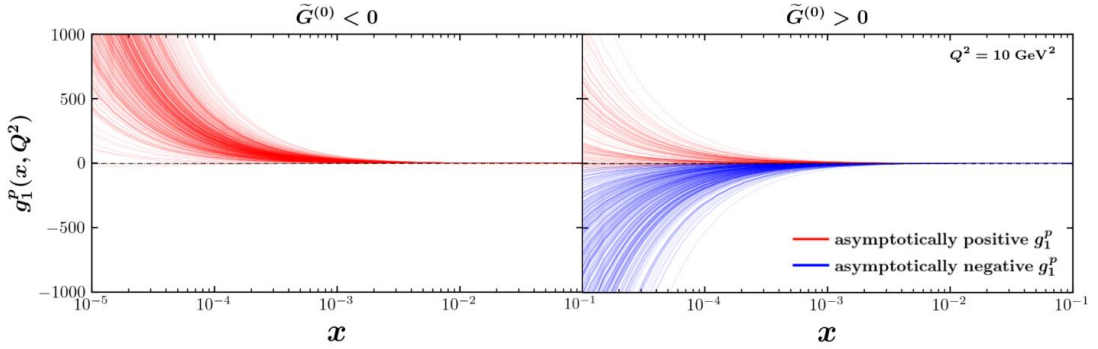

Asymptotic bimodality is caused by the insensitivity of DIS and SIDIS data to **gluon dominated dipole amplitudes** [7].

Global Analysis with pp Data

Polarized proton-proton collisions allow for leading order gluon-gluon interactions and thus can be more sensitive to the gluon dominated polarized dipole amplitudes.

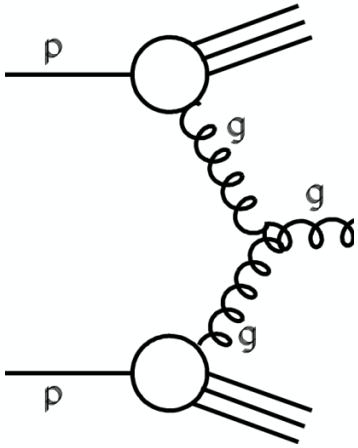

(Picture from CERN)

The polarized pp data available is $\boldsymbol{A_{LL}^{\text{jet}}}$, with jet cross-section [8]:

$$\frac{d\Delta\sigma^{pp\to\text{jet}X}}{d^2p_T^{\text{jet}}d\eta^{\text{jet}}} = \frac{1}{\pi S}\int_{x_g^{P,\min}}^1 \frac{dx_g^P}{x_g^P}\Delta f_g^P(x_g^P,\mu_F)\int_{x_g^{T,\min}}^1 \frac{dx_g^T}{x_g^T}\Delta f_g^T(x_g^T,\mu_F) \times \int_{z_g^{\min}}^1 \frac{dz_g}{z_g^2}\frac{d\Delta\hat{\sigma}_{gg}^g(\lambda,\hat{s},\hat{p_T},\hat{\eta},\mu_F,\mu_F',\mu_R)}{vdvdw}\mathcal{J}_g\left(z_g,\frac{Rp_T^{\text{jet}}}{\mu_F'},\mu_R\right)$$

DLA Accuracy: Only the leading order term in the jet function $\mathcal{J}_g$ preserves the resummation parameter $\alpha_s \ln^2(\frac{1}{x})$: $\boldsymbol{\mathcal{J}_g \equiv \delta(1-z_g)}$

The small-x cross-section **<u>in the pure-gluon limit</u>**:

$$\frac{\mathrm{d}\Delta\sigma^{pp\to\text{jet}X}}{\mathrm{d}^2p_T\mathrm{d}y} = \frac{8\,C_F}{\pi^3}\frac{1}{s\,p_T^2}\int_0^\infty \mathrm{d}x_\perp \frac{1}{\alpha_s(1/x_\perp^2)}\,x_\perp J_0(p_T\,x_\perp) \qquad \left(x_{T,P}\approx\frac{p_T}{\sqrt{s}}e^{\pm y}<0.1\right)$$

$$\times\left[2\,G_{2,P}\boldsymbol{\nabla}_\perp^2\widetilde{G}_T + 2\,(\boldsymbol{\nabla}_\perp^2\widetilde{G}_P)G_{2,T} + \frac{\partial}{\partial x_\perp}\widetilde{G}_P\frac{\partial}{\partial x_\perp}\widetilde{G}_T + 2\,\frac{\partial}{\partial x_\perp}G_{2,P}\frac{\partial}{\partial x_\perp}\widetilde{G}_T + 2\,\frac{\partial}{\partial x_\perp}\widetilde{G}_P\frac{\partial}{\partial x_\perp}G_{2,T}\right]$$

Influence of pp Data

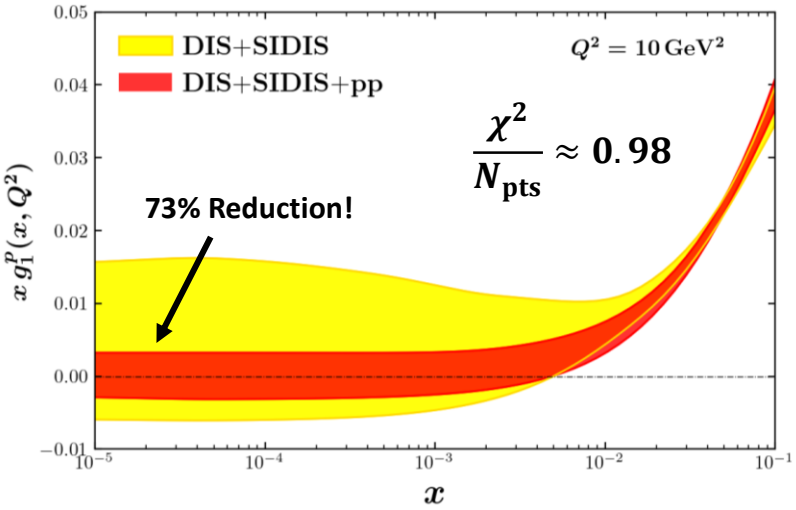

$$\Delta G(x,Q^2) = \frac{2N_c}{\alpha_s(Q^2)\pi^2} G_2(s_{10},\eta)\Big|_{\eta=\sqrt{\frac{N_c}{2\pi}}\ln\frac{Q^2}{x\Lambda^2}}^{s_{10}=\sqrt{\frac{N_c}{2\pi}}\ln\frac{Q^2}{\Lambda^2}}$$

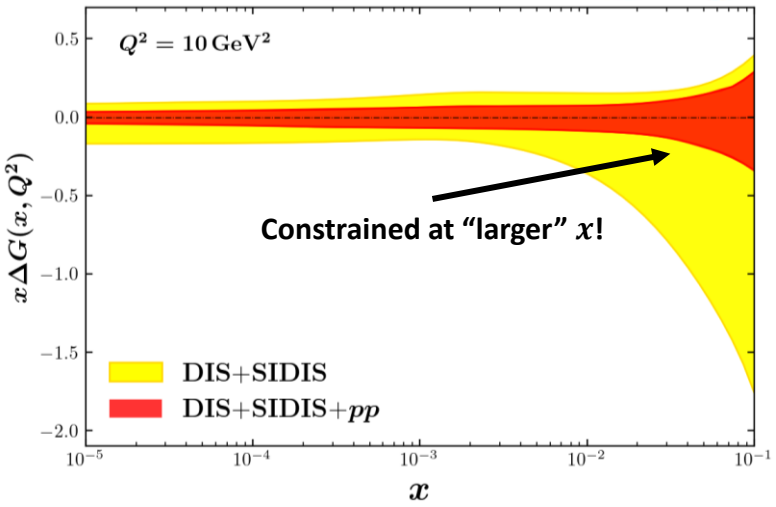

DIS+SIDIS: $S_{q+G}\Big|_{10^{-7}}^{0.1} = -0.52 \pm 0.90$

DIS+SIDIS+pp: $S_{q+G}\Big|_{10^{-7}}^{0.1} = -0.04 \pm 0.23$

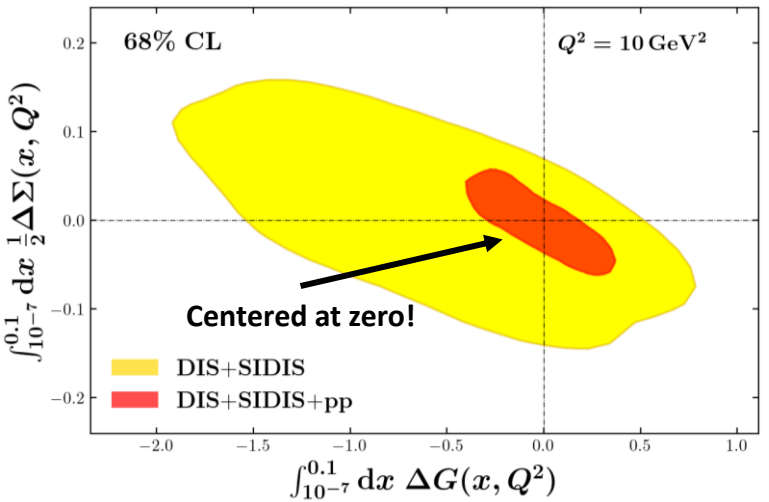

Uncertainty spans zero → Bimodality persists

EIC Impact Study

EIC Pseudo data: Create data points with EIC-consistent uncertainties/kinematics [10] using small-x theory input.

- $10^{-4} < x < 10^{-1}$, $1.69\ \mathrm{GeV}^2 < Q^2 < 50\ \mathrm{GeV}^2$
- Proton DIS: $\sqrt{s} = \{29, 45, 63, 141\}$ GeV, L = $100\ \mathrm{fb}^{-1}$
- Deuteron/^{3}He DIS: $\sqrt{s} = \{29, 66, 89\}$ GeV, L = $10\ \mathrm{fb}^{-1}$
- 2% point-to-point systematic uncertainty

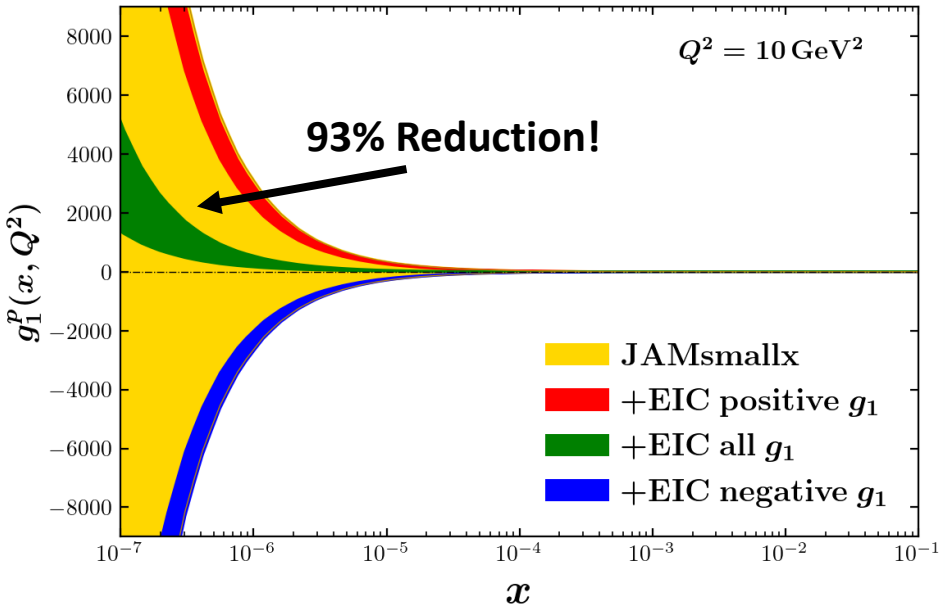

Final Thoughts

- Small-x helicity global analysis is successful and **not degraded** with the inclusion of polarized pp data.
- pp data drastically reduces uncertainty, especially for larger-x gluon hPDFs.
- Asymptotic bimodality persists → Can be broken with smaller-x data ($x \approx 10^{-4}$).
- Net quark and gluon spin <u>now consistent with zero:</u>
  - How will this be affected by re-introducing quarks?
  - Quark and gluon OAM contributions?

Interested? Check arXiv soon!
(also I'm available for a postdoc position!)

Bibliography

[1] R. L. Jaffe and A. Manohar,The G(1) Problem: Fact and Fantasy on the Spin of the Proton, Nucl. Phys. B337 (1990) 509–546.

[2] Y. V. Kovchegov, D. Pitonyak, and M. D. Sievert, Helicity Evolution at Small-x, J. High Energy Phys. 2016, 72 (2016).

[3] Y. V. Kovchegov and M. D. Sievert, Small-x Helicity Evolution: An Operator Treatment, Phys. Rev. D 99, 054032 (2019).

[4] Y. V. Kovchegov, D. Pitonyak, and M. D. Sievert, Helicity Evolution at Small x: Flavor Singlet and Non-Singlet Observables, Phys. Rev. D 95, 014033 (2017).

[5] F. Cougoulic, Y. V. Kovchegov, A. Tarasov, and Y. Tawabutr, Quark and Gluon Helicity Evolution at Small x: Revised and Updated, J. High Energy Phys. 2022, 95 (2022).

[6] D. Adamiak, Y. V. Kovchegov, W. Melnitchouk, D. Pitonyak, N. Sato, and M. D. Sievert, First Analysis of World Polarized DIS Data with Small-x Helicity Evolution, Phys. Rev. D 104, L031501 (2021).

[7] D. Adamiak et al., Global analysis of polarized DIS and SIDIS data with improved small-x helicity evolution, Phys. Rev. D. 108 (2023)

[8] Z.-B. Kang, F. Ringer, and I. Vitev, The semi-inclusive jet function in SCET and small radius resummation for inclusive jet production, JHEP 10, 125 (2016)

[9] Y. V. Kovchegov, M. Li, Gluon double-spin asymmetry in the longitudinally polarized $p + p$ collisions, JHEP 05, 177 (2024)

[10] R. Abdul Khalek et al., Science Requirements and Detector Concepts for the Electron-Ion Collider: EIC Yellow Report, Nucl. Phys. A 1026 (2022)

Extras

Cuts on Data

- We fit to all available DIS and SIDIS data within the kinematic ranges $5 \times 10^{-3} < x < 0.1$ and $1.69\ \mathrm{GeV}^2 < Q^2 < 10.4\ \mathrm{GeV}^2$
- This leaves a total of 240 data points in the JAM database.

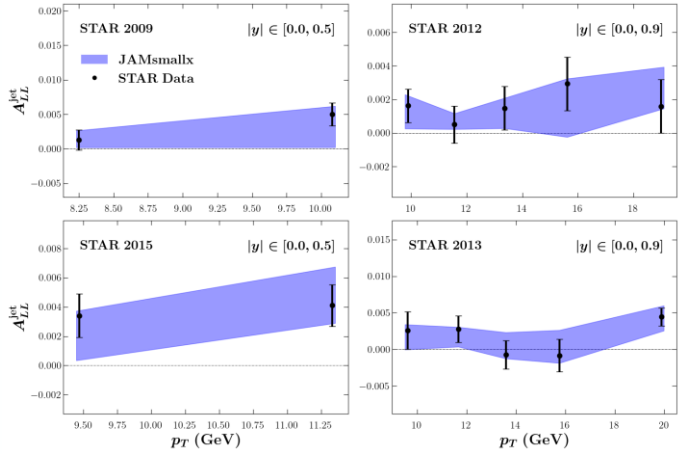

TABLE I. Summary of polarized DIS data included in the fit, separated into A_1 (left) and $A_\parallel$ (right), along with the χ^2/N_{pts} for each data set.

Data set (A_1)	Target	N_{pts}	χ^2/N_{pts}
COMPASS [120]	p	5	0.77
COMPASS [121]	p	17	0.93
COMPASS [122]	d	5	0.34
EMC [123]	p	5	0.23
HERMES [124]	n	2	1.11
SLAC (E142) [125]	^{3}He	1	1.47
SMC [126, 127]	p	6	1.26
	p	6	0.43
	d	6	0.65
	d	6	2.13
Total		59	0.90

Data set ($A_\parallel$)	Target	N_{pts}	χ^2/N_{pts}
HERMES [128]	p	4	1.47
	d	4	1.00
SLAC (E143) [129]	p	9	0.55
	d	9	1.01
SLAC (E154) [130]	^{3}He	5	0.69
SLAC(E155) [131]	p	16	1.07
	d	16	1.57
Total		63	1.10

TABLE II. Summary of the polarized SIDIS data on A_1^h included in the fit, along with the χ^2/N_{pts} for each data set.

Dataset (A_1^h)	Target	Tagged Hadron	N_{pts}	χ^2/N_{pts}
COMPASS [132]	d	π^+	5	0.63
	d	π^-	5	0.83
	d	h^+	5	1.01
	d	h^-	5	1.02
	d	K^+	5	1.60
	d	K^-	5	0.71
COMPASS [133]	p	π^+	5	1.94
	p	π^-	5	1.18
	p	K^+	5	0.46
	p	K^-	5	0.23
HERMES [134]	^{3}He	h^+	2	0.55
	^{3}He	h^-	2	0.29
HERMES [135]	p	π^+	2	2.75
	p	π^-	2	0.00
	p	h^+	2	1.25
	p	h^-	2	0.19
	d	π^+	2	0.58
	d	π^-	2	1.23
	d	h^+	2	3.03
	d	h^-	2	1.24
	d	K^+	2	0.82
	d	K^-	2	0.25
	d	$K^+ + K^-$	2	0.36
SMC [136]	p	h^+	7	1.22
	p	h^-	7	1.41
	d	h^+	7	0.84
	d	h^-	7	1.52
Total			104	1.04

TABLE III. Summary of polarized pp data on $A_{\mathrm{LL}}^{\mathrm{jet}}$ included in the fit along with the χ^2/N_{pts} for each data set.

Data set ($A_{\mathrm{LL}}^{\mathrm{jet}}$)	N_{pts}	χ^2/N_{pts}
STAR [137]	2	0.60
STAR [138]	5	0.30
STAR [139]	2	0.55
STAR [140]	5	0.24
Total	14	0.36

Extras

EIC impact: DGLAP extrapolation vs KPS-CTT prediction

- EIC pseudodata can break the bimodality, predicting a specific sign as $x \to 0$.
- Uncertainties in the extrapolation region are much smaller using small-x helicity than those using DGLAP evolution.